

Supplementary information

Preparation of electrochromic Prussian blue nanoparticles dispersible into various solvents for realisation of printed electronics

Manabu Ishizaki,^a Katsuhiko Kanaizuka,^a Makiko Abe,^a Yuji Hoshi,^a Masatomi Sakamoto,^{a,b} Tohru Kawamoto,^b Hisashi Tanaka,^b and Masato Kurihara ^{*a,b}

An insoluble solid of historic Prussian blue (PB) has been transformed into dispersible PB nanoparticles in water and various hydrophilic and hydrophobic organic solvents. Via hybrid surface modification using $\text{Na}_4[\text{Fe}^{\text{II}}(\text{CN})_6]$ and short-chain alkylamines, the insoluble PB was successfully dispersed in hydrophilic-and-hydrophobic boundary alcohols, such as *n*-butanol. The *n*-butanol-dispersible PB nanoparticles afforded homogeneous spin-coated thin films on various substrates. The chemisorbed shorter-chain alkylamines, *n*-propylamines, of the PB nanoparticles were thermally released at 100 °C from their surfaces to present stubborn electrochromic PB thin films adhering to the substrate via mutual coordination-bonding networks.

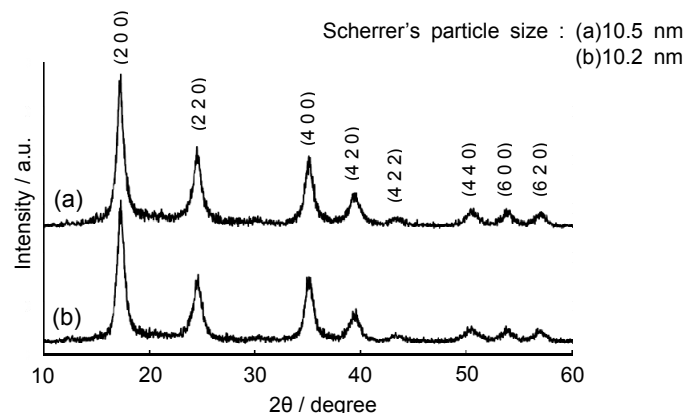


Fig. S1. XRD patterns of the original PB (insoluble PB NP solid) (a), the water-dispersible PB NP solid using $\text{Na}_4[\text{Fe}(\text{CN})_6]$ (b).

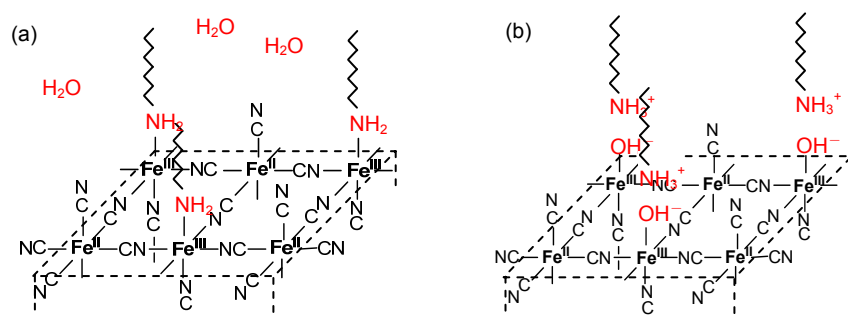


Fig. S2. Two types of surface modification using Fe(III)-OH₂ sites with alkylamines (R-NH₂).

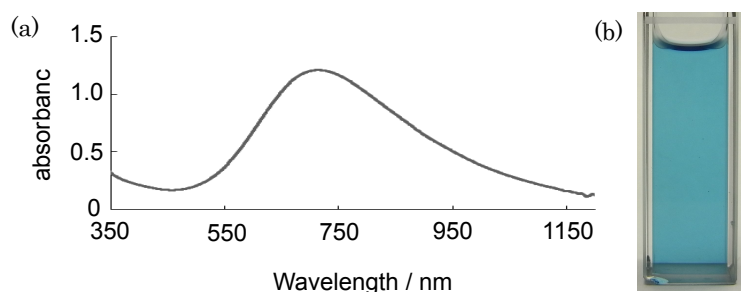


Fig S3. (a) UV-Vis-near IR absorption spectrum of the *n*-dodecylamine (C₁₂-amine)-modified PB NPs almost independently dispersed in *n*-butanol (78 µg / mL), and (b) a photograph of the blue dispersion solution with high transparency.

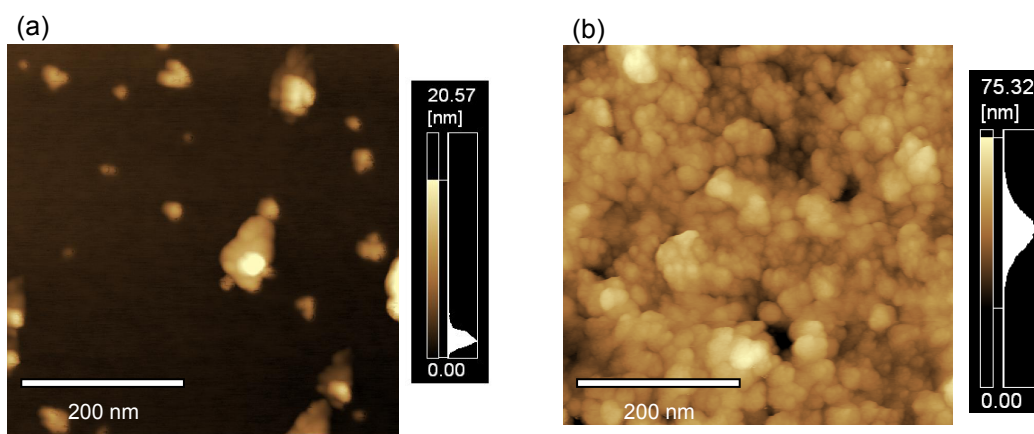


Fig. S4. AFM images of the spin-coated thin film using dilute (a) and dense (b) *n*-dodecylamine (C₁₂-amine)-modified PB NP inks.

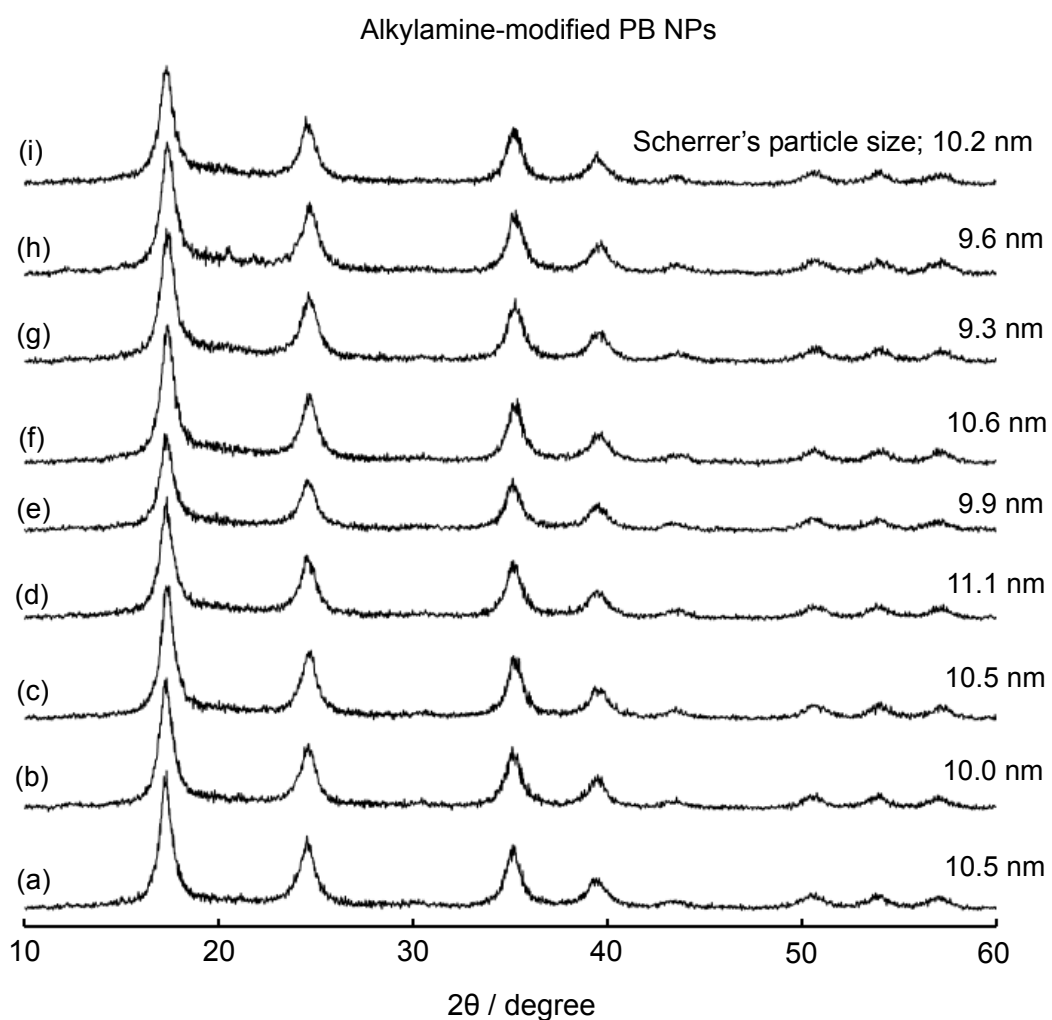


Fig. S5. Powder X-ray diffraction (XRD) patterns of (a) the original PB (insoluble PB NP solid), (b) *n*-propylamine-modified, (c) *n*-butylamine-modified, (d) *n*-hexylamine-modified, (e) *n*-octylamine-modified, (f) *n*-dodecylamine-modified, (g) *n*-hexadecylamine-modified, (h) *n*-octadecylamine-modified, (i) oleylamine-modified PB NP solids. The XRD patterns were recorded on Rigaku MiniFlex II desktop X-ray diffractometer ($\text{Cu K}\alpha_1$ radiation (1.540562 \AA)). The single-crystalline particle diameter (D) was calculated by the Scherrer's equation: $D = K\lambda/\beta\cos\theta$, where $K = 0.9$ (Scherrer's constant), λ = wavelength of X-ray, β = half band width, and θ = peak angle.

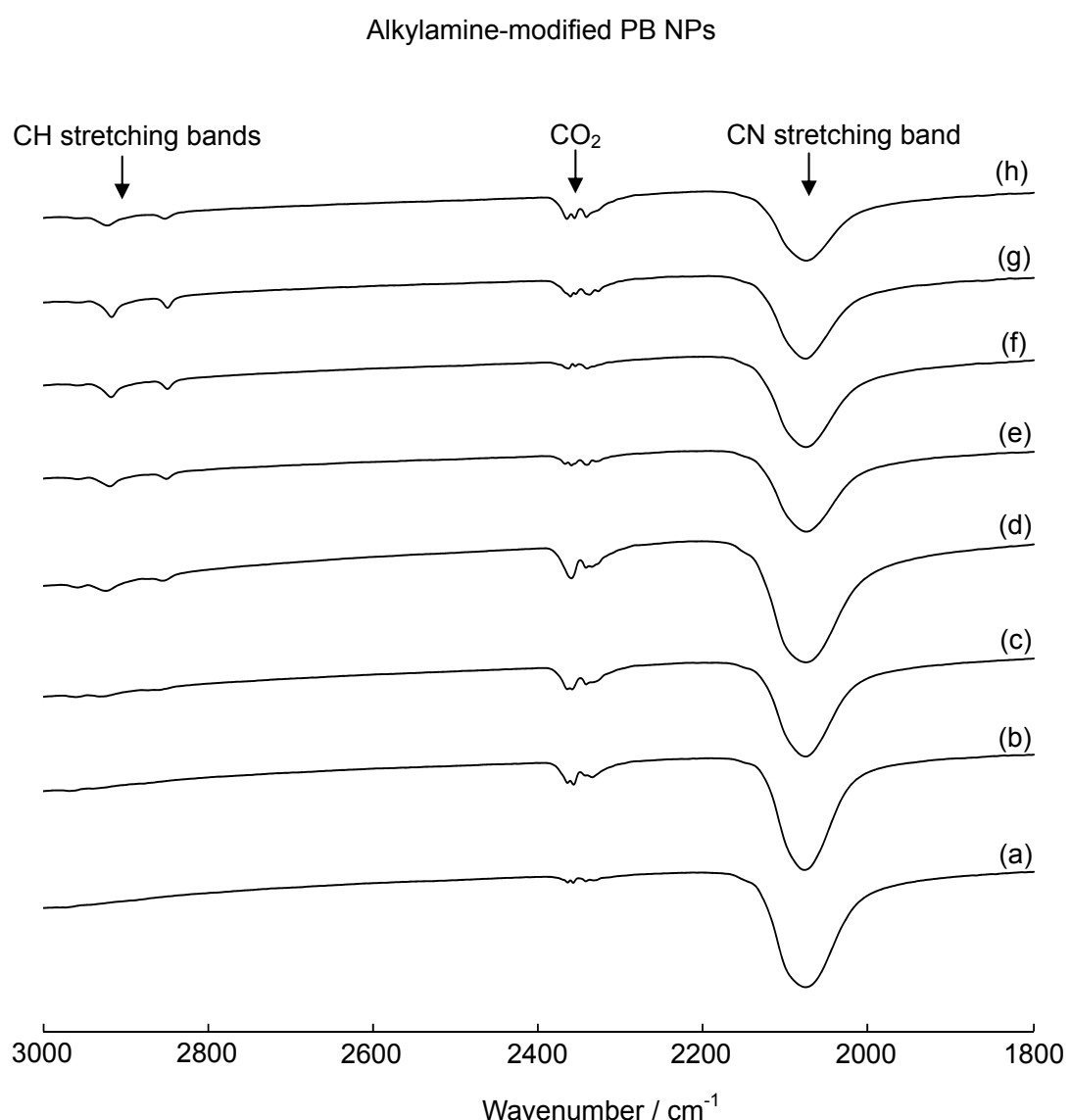


Fig. S6. FT-IR spectra of (a) *n*-propylamine-modified, (b) *n*-butylamine-modified, (c) *n*-hexylamine-modified, (d) *n*-octylamine-modified, (e) *n*-dodecylamine-modified, (f) *n*-hexadecylamine-modified, (g) *n*-octadecylamine-modified, (h) oleylamine-modified PB NP solids.

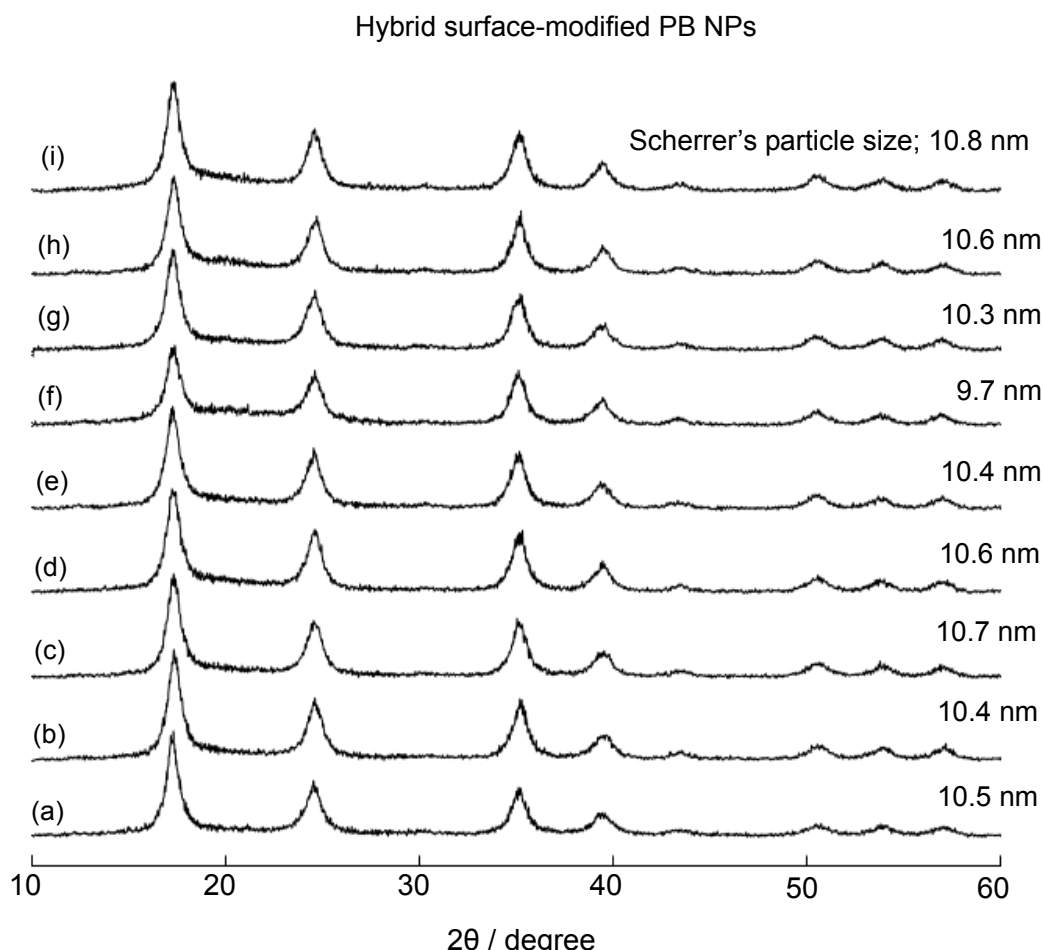


Fig. S7. Powder X-ray diffraction (XRD) patterns of (a) the original PB (insoluble PB NP solid), (b) *n*-propylamine-modified, (c) *n*-butylamine-modified, (d) *n*-hexylamine-modified, (e) *n*-octylamine-modified, (f) *n*-dodecylamine-modified, (g) *n*-hexadecylamine-modified, (h) *n*-octadecylamine-modified, (i) oleylamine-modified PB NP solids. The XRD patterns were recorded on Rigaku MiniFlex II desktop X-ray diffractometer ($\text{Cu K}\alpha_1$ radiation (1.540562 \AA)). The single-crystalline particle diameter (D) was calculated by the Scherrer's equation: $D = K\lambda/\beta\cos\theta$, where $K = 0.9$ (Scherrer's constant), λ = wavelength of X-ray, β = half band width, and θ = peak angle.

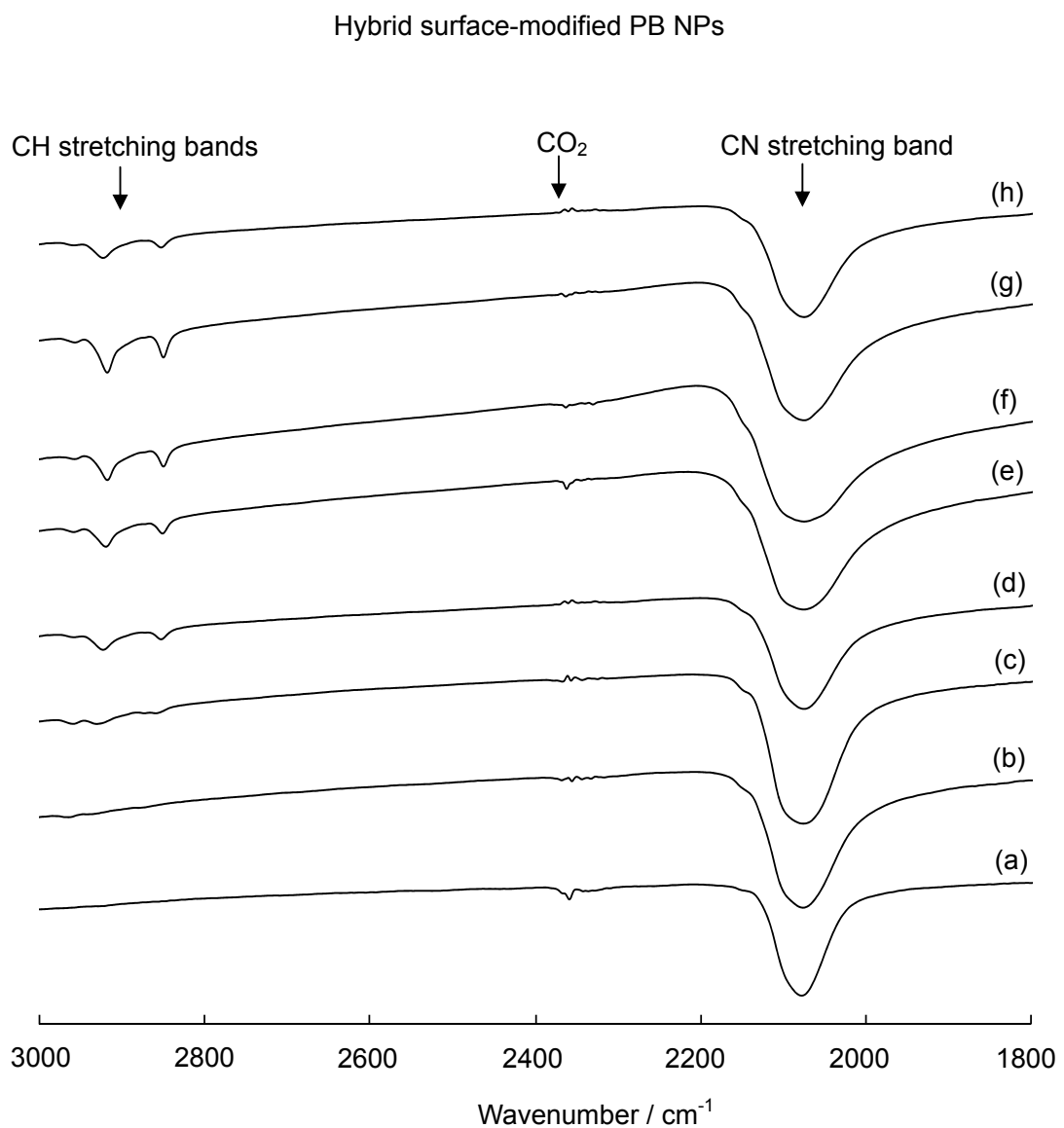


Fig. S8. FT-IR spectra of (a) *n*-propylamine-modified, (b) *n*-butylamine-modified, (c) *n*-hexylamine-modified, (d) *n*-octylamine-modified, (e) *n*-dodecylamine-modified, (f) *n*-hexadecylamine-modified, (g) *n*-octadecylamine-modified, (h) oleylamine-modified PB NP solids.

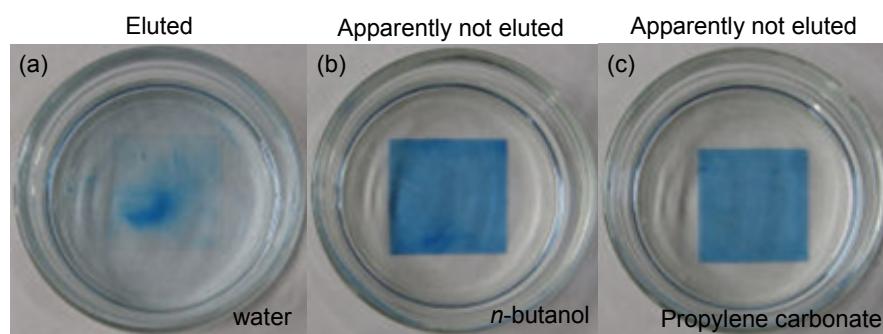


Fig. S9. Photographs of the PB NP thin film after drying at room temperature in (a) water, (b) *n*-butanol, and (c) propylene carbonate.

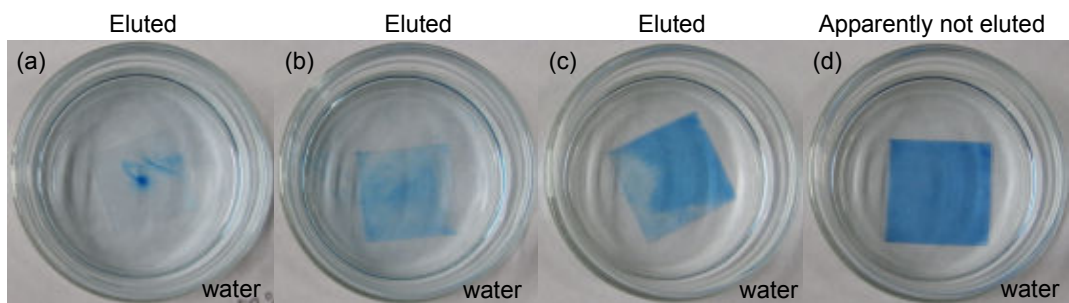


Fig. S10. Photographs of the PB NP thin film in water after heating (a) at 50°C for 10 min, (b) at 80°C for 10 min, (c) at 100°C for 10 min, and (d) at 100°C for 20 min.

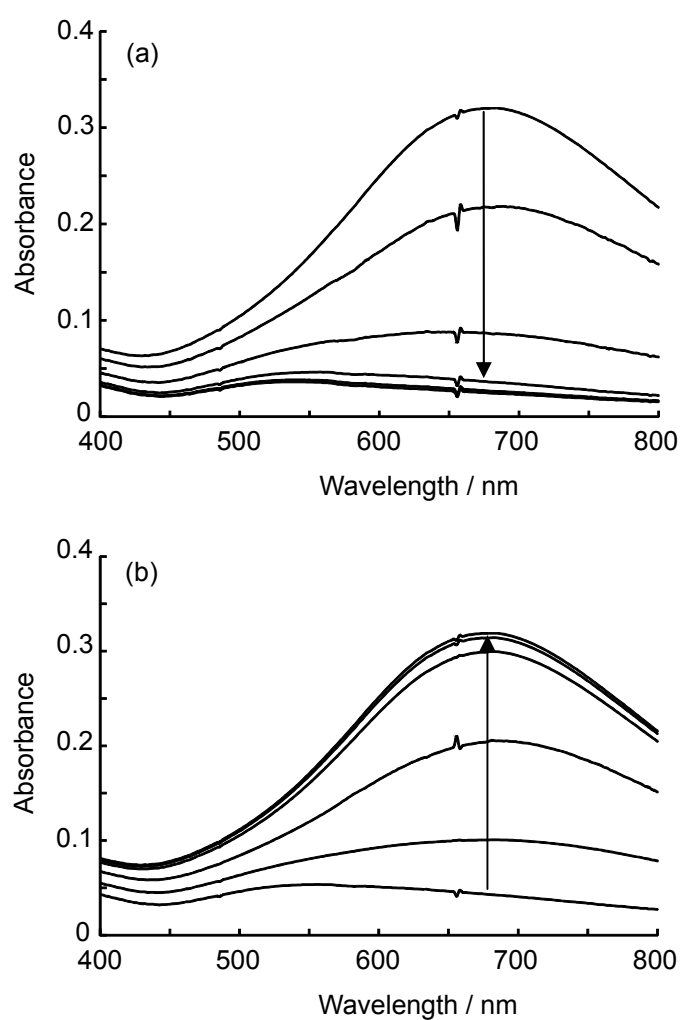


Fig. S10. Time-course change in the UV-vis absorption spectra of the PB NP film at -0.8 V (a) and 0.5 V (b) vs. Ag/Ag^+ .